BLIND QUALITY ASSESSMENT OF MULTIPLY-DISTORTED IMAGES BASED ON STRUCTURAL DEGRADATION

Tao Dai[⋆], *Ke Gu*[†], *Zhi-ya Xu*[⋆], *Qingtao Tang*[⋆], *Haoyi Liang*[‡], *Yong-bing Zhang*[⋆], *Shu-Tao Xia*[⋆]

[⋆]Graduate School at Shenzhen, Tsinghua University, Shenzhen, Guangdong, China
[†]Faculty of Information Technology, Beijing University of Technology, 100124, China
[‡]University of Virginia, Department of ECE, Charlottesville, VA, 22904, USA
Email: dait14@mails.tsinghua.edu.cn

ABSTRACT

It is known that images available usually undergo some stages of processing (e.g., acquisition, compression, transmission and display), and each stage may introduce certain type of distortion. Hence, images distorted by multiple types of distortions are common in real applications. Research in human visual perception has evidenced that the human visual system (HVS) is sensitive to image structural information. This fact inspires us to design a new blind/no-reference (NR) image quality assessment (IQA) method to evaluate the visual quality of multiply-distorted images based on structural degradation. Specifically, quality-aware features are extracted from both the first- and high-order image structures by local binary pattern (LBP) operators. Experimental results on two well-known multiply-distorted image databases demonstrate the outstanding performance of the proposed method.

Index Terms— Image quality assessment (IQA), no-reference (NR), multiple distortions, structural degradation, local binary pattern (LBP)

1. INTRODUCTION

Digital images are usually distorted by a wide variety of distortions during acquisition. Hence, image quality assessment (IQA) is a crucial issue in many practical applications [1, 2, 3, 4]. The goal of IQA is to provide computational models that reflect the quality of an image as perceived by human subjects.

Most existing IQA methods concentrate on estimating the visual quality of singly-distorted images, which is usually not true in general. In practice, digital images usually undergo several stages, and the processing of each stage may introduce certain distortions. For instance, the acquisition stage mainly introduces sensor noise, and the compression stage usually brings blockiness and blur artifacts. Therefore, it is common that images are distorted by multiple distortions. Compared with visual quality assessment for singly-distorted images, evaluate the visual quality of multiply-distorted images has more challenges. Chandler et al. [5] summarize the challenges of evaluating multiply-distorted images in three aspects: the influence of single distortions on image quality, the interaction between these distortions, and the joint effects of these distortions on the overall image quality. So, it is desirable to provide visual quality assessment methods of multiply-distorted images.

Recently, there exist some objective IQA methods designed for multiply-distorted images. In [6], the authors propose a six-step blind metric for multiply-distorted images by combining the single quality prediction of each emerging distortion type and joint effects of different distortion sources. In [7], natural scene statistics (NSS) features are combined to form an improved bag-of-words representation for quality prediction. More efficient methods [8, 9] measure potential structural degradations in gradient domain [8] or in perceptual opponent-color space [9]. Among them, the so-called gradient-weighted histogram of local binary pattern (GWH-GLBP) [8] applies the LBP [10] operator to extract the first-order (gradient information) structural features, and offers a higher generality. This is because the image structure carries important visual information from a scene, and also the human visual system (HVS) adaptively extracts structural information for image perception and understanding [11].

Motivated by the success in evaluating the visual quality based on structural degradation, we present a novel no-reference (NR) IQA method for multiply-distorted images based on structural degradation. Similar to GWH-GLBP, the proposed method predicts the image quality by measuring the structural degradation caused by multiple distortions. A number of quality-aware features are extracted from the gradient magnitude and contrast normalized maps, which represent the first- and high-order structural patterns of the distorted images, respectively. Then the rotation invariant uniform

This work is supported by the National Natural Science Foundation of China under grant Nos.61371078, 61375054, the R&D Program of Shenzhen under grant Nos. JCYJ20140509172959977,JSGG20150512162853495, ZDSYS20140509172959989, JCYJ20160331184440545, JCYJ20160513103916577, and the Guangdong Special Support program (2015TQ01X161).

LBP operator is adopted to extract the first-order structural patterns, while a generalized center-symmetric LBP (GCS-LBP) operator is proposed to extract high-order structural patterns due to the more complex characteristics.

Compared with GWH-GLBP, the main differences of the proposed method lie in two aspects: 1) GWH-GLBP only utilizes the first-order patterns (i.e., gradient information), whereas in the proposed method both the first- and high-order patterns are utilized for better extracting the image structural features; 2) GWH-GLBP adopts the simple Prewitt filters (3×3) to obtain gradient map which only considers two directions (horizontal and vertical) while the proposed method employs four directional high-pass filters (5×5) encompassing diagonal directions for image structure detection. Results of experiments demonstrate that our method obtains superior performance compared with state-of-the-art full-reference (FR) and NR IQA methods.

2. PROPOSED METHOD

The proposed method is designed according to the HVS's sensitivity to structural degradation. Motivated by the fact that HVS has separate mechanisms to process first- and high-order structural information [12], we extract such first- and high-order structural information of a given image in spatial domain. The first-order feature set is extracted from the gradient maps of distorted images. The high-order feature set is calculated in the normalized luminance maps of distorted images. The flowchart of the proposed method is in Fig. 1. It consists of two main stages: extracting of two sets of quality-aware features and support vector regression (SVR).

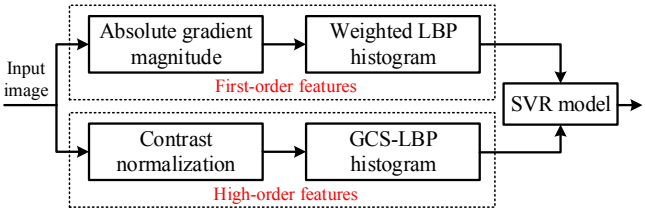

Fig. 1. Flowchart of the proposed method

A. First-order Features

Gradient information is the first-order image structures that characterize image local luminance changes, and conveys important visual information [13]. The simple Sobel or Prewitt operators are widely adopted to extract first-order image structures for blind IQA tasks [8]. However, these kernels are often too small (3×3) to include sufficient neighboring information and only two directions (horizontal and vertical) are considered. To extract more neighboring information including diagonal directions, we adopt four directional high-pass filters M_k $(k = 1, 2, 3, 4)$, as shown in Fig. 2.

The gradient magnitudes of a distorted image are computed as the maximum weighted average of difference for the block as:

$$G(i,j) = \max_{k=1,2,3,4} \text{mean2}(|I \otimes M_k|)(i,j), \tag{1}$$

where i and j denote the spatial indices of the image; $|\cdot|$ denotes the absolute value operator; I and G denote the distorted image and its corresponding gradient magnitude map; the symbol "$\otimes$" denotes the convolution operation; mean2$(\cdot)$ denotes the average value of a matrix.

0	0	0	0	0
1	3	8	3	1
0	0	0	0	0
-1	-3	-8	-3	-1
0	0	0	0	0

M1

0	0	1	0	0
0	8	3	0	0
1	3	0	-3	-1
0	0	-3	-8	0
0	0	-1	0	0

M2

0	0	1	0	0
0	0	3	8	0
-1	-3	0	3	1
0	-8	-3	0	0
0	0	-1	0	0

M3

0	1	0	-1	0
0	3	0	-3	0
0	8	0	-8	0
0	3	0	-3	0
0	1	0	-1	0

M4

Fig. 2. Operators for calculating the gradient value

After that, the LBP operator is used to extract the image local structures in the gradient magnitude map. The basic LBP operator for each coefficient in the gradient magnitude map can be expressed as

$$\text{LBP}_{P,R}(G_c) = \sum_{p=0}^{P-1} s(G_p - G_c)2^p, \tag{2}$$

where P and R are the number of neighbors and the radius of the neighborhood; G_c and G_p are the gradient magnitudes at the center of neighborhood and its neighbor; $s(x)$ is a sign function formed by $s(x) = \begin{cases} 1, & x \geq 0 \\ 0, & \text{otherwise.} \end{cases}$

To obtain rotation invariance, a histogram of the LBP codes (length $P + 2$) derived from a rotation-invariant and uniform variant of LBP operator can be defined as

$$\text{LBP}^{\text{riu2}}_{P,R} = \begin{cases} \sum_{p=0}^{P-1} s(G_p - G_c), & \text{if } \mathcal{U}(\text{LBP}_{P,R}) \leq 2 \\ P+1 & \text{otherwise} \end{cases} \tag{3}$$

where $\mathcal{U}$ is the uniform measure that calculates the number of bitwise transitions, and a rotation-invariant and uniform variant of LBP has $\mathcal{U}$ less than 2.

Although $\text{LBP}^{\text{riu2}}_{P,R}$ provides an effective feature vector to describe the image structure, it only encodes the sign of the differences (between the value of the central pixel and its neighbors). As shown in [14], the magnitude components of the differences also contribute to additional discriminant information. To encode such information, we use the gradient magnitude as the $\text{LBP}^{\text{riu2}}_{P,R}$ weight of each pixel, the normalized gradient-weighted LBP histogram is formulated as

$$H_{\text{LBP}}(h) = \frac{\sum_{i=1}^{M}\sum_{j=1}^{N} G(i,j) \cdot f(\text{LBP}^{\text{riu2}}_{P,R}(G(i,j)), h)}{\sum_{i=1}^{M}\sum_{j=1}^{N} G(i,j)}, \tag{4}$$

where

$$f(x,y) = \begin{cases} 1, & x = y \\ 0, & \text{otherwise}, \end{cases} \tag{5}$$

where M and N denote the image size; $h \in [0, P+1]$ is the possible LBP patterns and the gradient magnitude $G(i,j)$ is assigned to the weight of LBP histogram. In such a way, we can extract the first-order image structures with high-contrast changes.

B. High-order Features

Besides the first-order image structures obtained by the gradient-weighted $\text{LBP}^{\text{riu2}}_{P,R}$ as stated above, natural images also contain high-order structures (e.g. texture), which cannot be detected by the simple linear filters [12]. To extract such image structures, global contrast normalization is adopted to reduce contrast and luminance variations by mean subtraction and divisive normalization. Such an operation is applied to intensity image I to produce the normalized version $\hat{I}$,

$$\hat{I}(i,j) = \frac{I(i,j) - \mu}{\sigma + const}, \tag{6}$$

where i and j are the spatial indices of the image, $const$ is a small number to avoid division-by-zero, and the global mean and standard deviation of the whole image are defined as

$$\mu = \frac{1}{MN} \sum_{i=1}^{M} \sum_{j=1}^{N} I(i,j), \tag{7}$$

$$\sigma = \sqrt{\frac{1}{MN} \sum_{i=1}^{M} \sum_{j=1}^{N} (I(i,j) - \mu)^2}. \tag{8}$$

After global contrast normalization, we propose a generalized center-symmetric LBP (GCS-LBP) operator to extract the high-order features in $\hat{I}$ due to its more complex characteristics. The GCS-LBP encoding map is defined as

$$\text{GCS-LBP}_{R,P,T} = \sum_{p=0}^{P/2-1} \hat{s}(|\hat{I}_p - \hat{I}_{p+(P/2)}|) 2^p, \tag{9}$$

where $\hat{I}_p$ and $\hat{I}_{p+(P/2)}$ denote the grayvalues of center-symmetric pairs of pixels of P equally spaced pixels on a circle of radius of R; the function $\hat{s}(\cdot)$ is defined as $\hat{s}(x) = \begin{cases} 1, & x > T \\ 0, & \text{otherwise}, \end{cases}$ where T is a small threshold value. Note that GCS-LBP has only $2^{P/2}$ histogram bins, which is much less than that in the standard LBP (2^P bins).

Compared with the standard LBP, the proposed GCS-LBP has two advantages: 1) it is more robust to lumination changes due to the use of threshold T; 2) it captures better gradient information than the basic LBP, because instead of comparing the gray-level of each pixel with the center pixel, gray-level differences between center-symmetric pairs of pixels in a neighborhood are computed.

C. Regression Model for Quality Prediction

For LBP and GCS-LBP operators, the number of neighbors P is 8, and the radius of the neighborhood R is 1, thus producing 10 and 16 histogram bins, respectively. The value of threshold T set as 0.1 empirically. To consider varying viewing distance and image resolution [15], the $\text{LBP}^{\text{riu2}}_{(P,R)}$ and $\text{GCS-LBP}_{R,P,T}$ histograms are extracted in three scales, and the coarser scale is constructed by low-pass filtering and downsampling the image by a factor of two. Thus, the extracted features have 78 components in total.

After obtaining features, a mapping is required for feature pooling from the feature space to a quality index. In this work, the support vector regression (SVR) [16] with radial basis function (RBF) is adopted as the mapping function.

3. EXPERIMENTAL RESULTS

A.Database Description and Evaluation Criteria

We have tested the proposed method on two well-known multiply-distorted databases, MLIVE [17] and MDID2013 [6]. The MLIVE database consists of two subsets. The first subset contains 15 reference images distorted by Gaussian blur (GB) followed by JPEG compression. The second subset contains the same reference images distorted by GB followed by white noise (WN). In total, MLIVE has 450 distorted images. The MDID2013 database includes 324 distorted images created from 12 reference image. Each of reference image is distorted by three types of distortions (GB+JPEG+WN).

Three performance criteria, Spearman rank-order correlation coefficient (SRCC), Pearson linear correlation coefficient (PLCC) and root mean square error (RMSE), are adopted to evaluate the performance of IQA methods. The PLCC and RMSE are computed after the monotonic logistic mapping. A better IQA index has higher SRCC and PLCC, and lower RMSE values. For SVR learning on each database, distorted images of 80% of the reference images are selected for training, and the rest are used for testing. This random training-testing trial is repeated 1000 times, and the median performance is reported.

B. Performance Comparison with FR-IQA Methods

We compared the proposed method with 14 prominent FR-IQA methods including PSNR, VSNR [18], NQM [19], SSIM [11], IW-SSIM [20], OSS-SSIM [21], VIF [22], MAD [23], ADM [24], FSIM [25], GMS [13], IGM [26], VSI [27], GMSD [28]. All the results are listed in Table 1. From these results, the best two FR-IQA methods on MLIVE database are NQM and VIF, while on MDID2013, the top two FR-IQA methods are IW-SSIM and VIF. Besides, the performance of all methods on MDID2013 is inferior to their corresponding performance on MLIVE. This is because that the distorted image in MDID2013 are distorted by three types of distortions

Table 1. Performance comparison with state-of-the-art FR-IQA methods. The best results are highlighted in bold.

IQA method	MLIVE (450 images)			MDID2013 (324 images)		
	SRCC	PLCC	RMSE	SRCC	PLCC	RMSE
PSNR	0.728	0.817	10.870	0.644	0.653	0.035
VSNR	0.828	0.882	8.883	0.635	0.656	0.035
NQM	0.924	0.930	6.795	0.715	0.695	0.034
SSIM	0.903	0.927	6.967	0.622	0.656	0.036
IW-SSIM	0.911	0.939	6.636	0.888	0.887	0.023
OSS-SSIM	0.919	0.931	6.682	0.764	0.731	0.034
VIF	0.914	0.932	6.761	0.906	0.915	0.021
MAD	0.895	0.915	7.606	0.857	0.862	0.023
ADM	0.909	0.924	7.050	0.830	0.849	0.025
FSIM	0.895	0.917	7.039	0.750	0.770	0.031
GMS	0.887	0.914	7.430	0.786	0.804	0.028
IGM	0.888	0.924	7.195	0.878	0.882	0.022
VSI	0.878	0.910	7.655	0.730	0.744	0.031
GMSD	0.880	0.912	7.656	0.877	0.902	0.021
Ours	**0.952**	**0.956**	**5.479**	**0.923**	**0.935**	**0.017**

whereas the distorted images in MLIVE are distorted by two types of distortions. Compared with the proposed method, all the compared FR-IQA methods obtain lower results on both databases.

C. Performance Comparison with NR-IQA Methods

Table 2. Performance comparison with state-of-the-art NR-IQA methods. The symbol "*" denotes the proposed method are statistically better than the corresponding methods. The best results are highlighted in bold.

IQA method	MLIVE			MDID2013			ET(s)
	SRCC	PLCC	RMSE	SRCC	PLCC	RMSE	
BIQI	0.884*	0.905	7.831	0.863*	0.883	0.023	0.45
NIQE	0.789*	0.858	9.489	0.614*	0.645	0.037	0.41
ILNIQE	0.901*	0.914	7.538	0.707*	0.709	0.034	7.59
BLIINDS2	0.888*	0.904	7.981	0.808*	0.844	0.027	55.21
DIIVINE	0.866*	0.899	8.256	0.836*	0.846	0.027	17.41
CORNIA	0.901*	0.917	7.587	0.898*	0.905	0.020	2.46
BRISQUE	0.900*	0.924	7.143	0.819*	0.833	0.027	0.08
GMLOG	0.834*	0.873	9.165	0.825*	0.831	0.026	0.06
NFERM	0.898*	0.917	7.459	0.855*	0.871	0.024	50.96
SISBLM	0.907*	0.925	7.194	0.886*	0.885	0.023	3.71
GWH-GLBP	0.941*	0.947	5.919	0.903*	0.912	0.020	0.13
Ours	**0.952**	**0.956**	**5.479**	**0.923**	**0.935**	**0.017**	0.21

The proposed method is also compared with 11 prominent NR-IQA methods including BIQI [29], NIQE [30], ILNIQE [31], BLIINDS2 [32], DIIVINE [33], CORNIA [34], BRISQUE [15], GMLOG [35], NFERM [36], SISBLM [6], GWH-GLBP [8]. Among them, NIQE and ILNIQE are unsupervised methods without training while the others including the proposed method require training-testing trials. The source codes of the compared NR-IQA methods are derived from their original authors. All the results of these methods are reported in Table 2. From these results, we can see that the proposed method, GWH-GLBP and SISBLM are the top three three NR-IQA methods on both databases. This is because that these three methods are specifically designed for evaluating multiply-distorted images while others are general-purpose NR-IQA methods. Despite the wonderful performance of GWH-GLBP by extracting the first-order image structures, it is still slightly inferior to the proposed method. The reason is that our method extracts more structural information including both the first- and high-order image structures.

In order to evaluate statistical significance, we perform two sample T-test (significance level 0.05) between SRCC by the compared NR-IQA methods across 1000 trials. The results are listed in Table 2, where the symbol "*" denotes that the proposed method are statistically better than the corresponding NR-IQA methods. As shown in Table 2, it can be seen that the proposed method performs better than all the compared NR-IQA methods on both databases.

Besides, we also validate the effect of the four-directional gradient operator we use. In experiments, we test our method with the simple two-directional Prewitt operator and the four-directional operator on MLIVE. The median SRCC across 1000 train-test trials of the proposed method with each of two operators are 0.944 and 0.952, respectively. Thus, using the four-directional gradient operator provides a better accuracy.

In Table 2, we also report the average execution time (the last column) of the feature extraction by each NR-IQA method. The experiments are performed on a sample 768×512 in Matlab on an Inter Core i5-3470 CPU @3.2 GHz. The results show that the proposed method with its unoptimized code ranks fourth in the list, which demonstrates its efficiency for IQA task.

4. CONCLUSIONS

In this paper, we propose an efficient NR-IQA method to predict the visual quality of multiply-distorted images based on structural degradation. In the proposed method, image structural features are extracted from gradient and luminance normalized maps to characterize the image first-order and high-order structural information. The proposed method has been compared with several prominent FR- and NR-IQA methods on two public multiply-distorted image databases. Experimental results demonstrate the outstanding performance of the proposed method in terms of prediction accuracy with relatively low computational complexity.

5. REFERENCES

[1] H. Liang and D. S. Weller, "Comparison-based image quality assessment for selecting image restoration parameters," *IEEE Transactions on Image Processing*, vol. 25, no. 11, pp. 5118–5130, Nov 2016.

[2] K. Gu, D. Tao, J. F. Qiao, and W. Lin, "Learning a no-reference quality assessment model of enhanced images with big data," *IEEE Transactions on Neural Networks and Learning Systems*, vol. PP, no. 99, pp. 1–13, 2017.

[3] Tao Dai, Chao-Bing Song, Ji-Ping Zhang, and Shu-Tao Xia, "Pmpa: A patch-based multiscale products algorithm for image denoising," in *Image Processing (ICIP), 2015 IEEE International Conference on*. IEEE, 2015, pp. 4406–4410.

[4] Tao Dai, Weizhi Lu, Wei Wang, Jilei Wang, and Shu-Tao Xia, "Entropy-based bilateral filtering with a new range kernel," *Signal Processing*, vol. 137, pp. 223 – 234, 2017.

[5] Damon M Chandler, "Seven challenges in image quality assessment: past, present, and future research," *ISRN Signal Processing*, vol. 2013, 2013.

[6] Ke Gu, Guangtao Zhai, Xiaokang Yang, and Wenjun Zhang, "Hybrid no-reference quality metric for singly and multiply distorted images," *IEEE Transactions on Broadcasting*, vol. 60, no. 3, pp. 555–567, 2014.

[7] Yanan Lu, Fengying Xie, Tongliang Liu, Zhiguo Jiang, and Dacheng Tao, "No reference quality assessment for multiply-distorted images based on an improved bag-of-words model," *IEEE Signal Processing Letters*, vol. 22, no. 10, pp. 1811–1815, 2015.

[8] Qiaohong Li, Weisi Lin, and Yuming Fang, "No-reference quality assessment for multiply-distorted images in gradient domain," *IEEE Signal Processing Letters*, vol. 23, no. 4, pp. 541–545, 2016.

[9] Hadi Hadizadeh and Ivan V Bajić, "Color gaussian jet features for no-reference quality assessment of multiply-distorted images," *IEEE Signal Processing Letters*, vol. 23, no. 12, pp. 1717–1721, 2016.

[10] Timo Ojala, Matti Pietikäinen, and Topi Mäenpää, "Multiresolution gray-scale and rotation invariant texture classification with local binary patterns," *Pattern Analysis and Machine Intelligence, IEEE Transactions on*, vol. 24, no. 7, pp. 971–987, 2002.

[11] Zhou Wang, Alan Conrad Bovik, Hamid Rahim Sheikh, and Eero P Simoncelli, "Image quality assessment: from error visibility to structural similarity," *Image Processing, IEEE Transactions on*, vol. 13, no. 4, pp. 600–612, 2004.

[12] Jonas Larsson, Michael S Landy, and David J Heeger, "Orientation-selective adaptation to first-and second-order patterns in human visual cortex," *Journal of neurophysiology*, vol. 95, no. 2, pp. 862–881, 2006.

[13] Anmin Liu, Weisi Lin, and Manish Narwaria, "Image quality assessment based on gradient similarity," *IEEE Transactions on Image Processing*, vol. 21, no. 4, pp. 1500–1512, 2012.

[14] Zhenhua Guo, Lei Zhang, and David Zhang, "A completed modeling of local binary pattern operator for texture classification," *Image Processing, IEEE Transactions on*, vol. 19, no. 6, pp. 1657–1663, 2010.

[15] Anish Mittal, Anush Krishna Moorthy, and Alan Conrad Bovik, "No-reference image quality assessment in the spatial domain," *Image Processing, IEEE Transactions on*, vol. 21, no. 12, pp. 4695–4708, 2012.

[16] Bernhard Schölkopf and Alexander J Smola, *Learning with kernels: Support vector machines, regularization, optimization, and beyond*, MIT press, 2002.

[17] Dinesh Jayaraman, Anish Mittal, Anush K Moorthy, and Alan C Bovik, "Objective quality assessment of multiply distorted images," in *2012 Conference Record of the Forty Sixth Asilomar Conference on Signals, Systems and Computers (ASILOMAR)*. IEEE, 2012, pp. 1693–1697.

[18] Damon M Chandler and Sheila S Hemami, "Vsnr: A wavelet-based visual signal-to-noise ratio for natural images," *Image Processing, IEEE Transactions on*, vol. 16, no. 9, pp. 2284–2298, 2007.

[19] Niranjan Damera-Venkata, Thomas D Kite, Wilson S Geisler, Brian L Evans, and Alan C Bovik, "Image quality assessment based on a degradation model," *IEEE transactions on image processing*, vol. 9, no. 4, pp. 636–650, 2000.

[20] Zhou Wang and Qiang Li, "Information content weighting for perceptual image quality assessment," *Image Processing, IEEE Transactions on*, vol. 20, no. 5, pp. 1185–1198, 2011.

[21] Ke Gu, Min Liu, Guangtao Zhai, Xiaokang Yang, and Wenjun Zhang, "Quality assessment considering viewing distance and image resolution," *IEEE Transactions on Broadcasting*, vol. 61, no. 3, pp. 520–531, 2015.

[22] Hamid Rahim Sheikh and Alan C Bovik, "Image information and visual quality," *Image Processing, IEEE Transactions on*, vol. 15, no. 2, pp. 430–444, 2006.

[23] Eric C Larson and Damon M Chandler, "Most apparent distortion: full-reference image quality assessment and the role of strategy," *Journal of Electronic Imaging*, vol. 19, no. 1, pp. 011006–011006, 2010.

[24] Songnan Li, Fan Zhang, Lin Ma, and King Ngi Ngan, "Image quality assessment by separately evaluating detail losses and additive impairments," *IEEE Transactions on Multimedia*, vol. 13, no. 5, pp. 935–949, 2011.

[25] Lin Zhang, Lei Zhang, Xuanqin Mou, and David Zhang, "Fsim: a feature similarity index for image quality assessment," *Image Processing, IEEE Transactions on*, vol. 20, no. 8, pp. 2378–2386, 2011.

[26] Jinjian Wu, Weisi Lin, Guangming Shi, and Anmin Liu, "Perceptual quality metric with internal generative mechanism," *IEEE Transactions on Image Processing*, vol. 22, no. 1, pp. 43–54, 2013.

[27] Lin Zhang, Ying Shen, and Hongyu Li, "Vsi: A visual saliency-induced index for perceptual image quality assessment," *IEEE Transactions on Image Processing*, vol. 23, no. 10, pp. 4270–4281, 2014.

[28] Wufeng Xue, Lei Zhang, Xuanqin Mou, and Alan C Bovik, "Gradient magnitude similarity deviation: a highly efficient perceptual image quality index," *Image Processing, IEEE Transactions on*, vol. 23, no. 2, pp. 684–695, 2014.

[29] Anush Krishna Moorthy and Alan Conrad Bovik, "A two-step framework for constructing blind image quality indices," *IEEE Signal Processing Letters*, vol. 17, no. 5, pp. 513–516, 2010.

[30] Anish Mittal, Rajiv Soundararajan, and Alan C Bovik, "Making a completely blind image quality analyzer," *IEEE Signal Processing Letters*, vol. 20, no. 3, pp. 209–212, 2013.

[31] Lin Zhang, Lei Zhang, and Alan C Bovik, "A feature-enriched completely blind image quality evaluator," *IEEE Transactions on Image Processing*, vol. 24, no. 8, pp. 2579–2591, 2015.

[32] Michele A Saad, Alan C Bovik, and Christophe Charrier, "Blind image quality assessment: A natural scene statistics approach in the dct domain," *IEEE Transactions on Image Processing*, vol. 21, no. 8, pp. 3339–3352, 2012.

[33] Anush Krishna Moorthy and Alan Conrad Bovik, "Blind image quality assessment: From natural scene statistics to perceptual quality," *IEEE Transactions on Image Processing*, vol. 20, no. 12, pp. 3350–3364, 2011.

[34] Peng Ye, Jayant Kumar, Le Kang, and David Doermann, "Unsupervised feature learning framework for no-reference image quality assessment," in *Computer Vision and Pattern Recognition (CVPR), 2012 IEEE Conference on*. IEEE, 2012, pp. 1098–1105.

[35] Min Zhang, Chisako Muramatsu, Xiangrong Zhou, Takeshi Hara, and Hiroshi Fujita, "Blind image quality assessment using the joint statistics of generalized local binary pattern," *IEEE Signal Processing Letters*, vol. 22, no. 2, pp. 207–210, 2015.

[36] Ke Gu, Guangtao Zhai, Xiaokang Yang, and Wenjun Zhang, "Using free energy principle for blind image quality assessment," *IEEE Transactions on Multimedia*, vol. 17, no. 1, pp. 50–63, 2015.